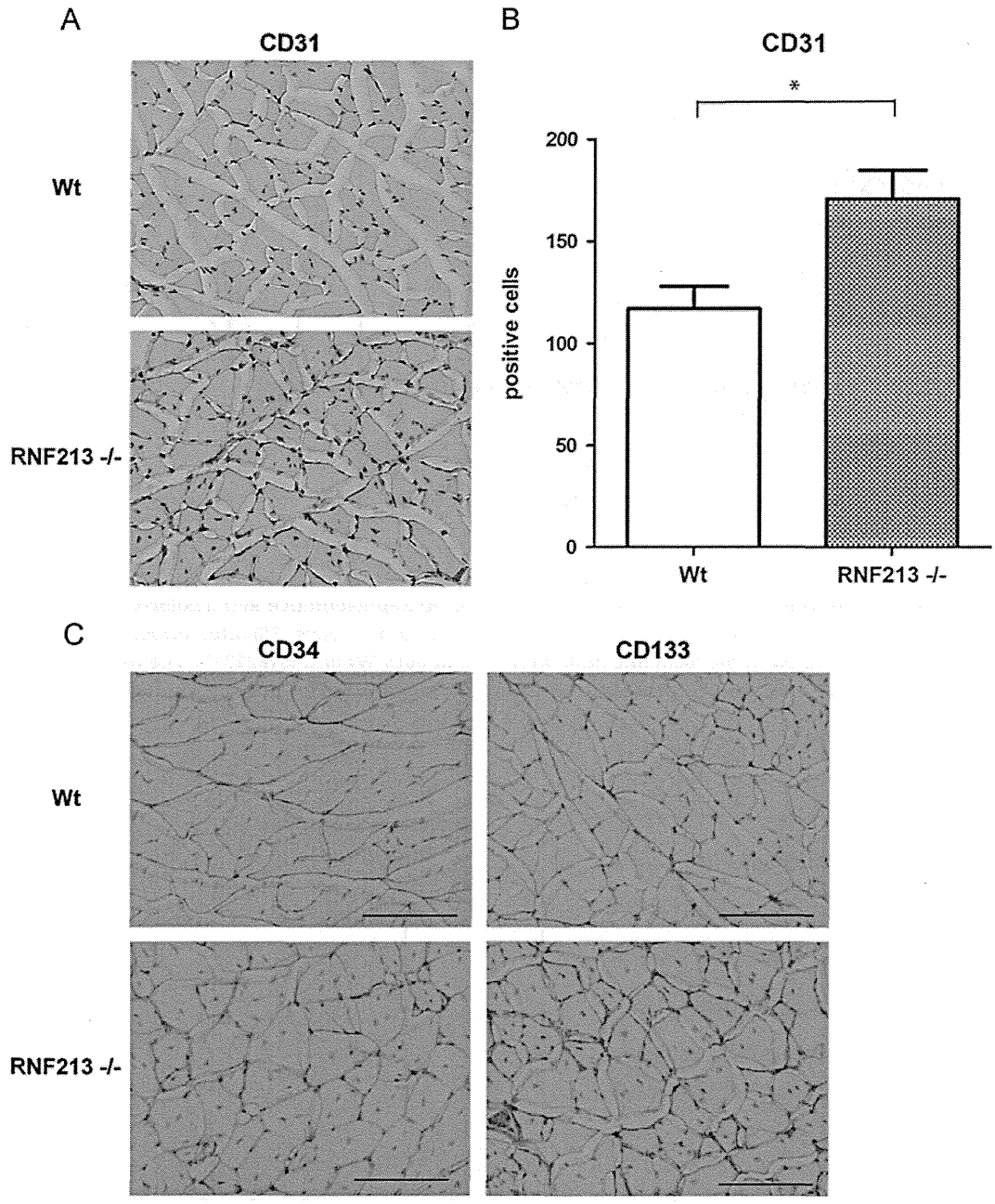

Fig. 6 – Vascular density in the GC muscle 28 days after femoral artery ligation. (A) Representative micrographs of the GC muscle in Wt and RNF213-/-. Vascular endothelial cells were positively stained by the anti-CD31 antibody. (B) Vascular density in the GC muscle was significantly higher in RNF213-/- than in Wt. (GC, gastrocnemius; *$p<0.05$.) The immunohistochemistry for CD34 and CD133 were also performed to evaluate angiogenesis and stem cell expression (C), both of which were completely in accordance with the result of CD31.

model of chronic cerebral ischemia that reproducibly leads to angiogenesis at the base of the brain, we employed two types of ischemia models in mice; tMCAO and the hind-limb ischemia model by femoral artery ligation. Although tMCAO is an acute ischemia model, we evaluated angiogenic responses at the base of the brain, which is the vascular territory of ischemia in this model, in the chronic state. Although permanent MCAO could be the alternative model in light of its chronic ischemic pathology in the ischemic penumbra of long-term survivors, mortality rate of permanent MCAO in C57BL/6 mice is extremely high and we finally employed tMCAO model. The failure to detect any significant difference in angiogenesis between RNF213 -/- and Wt could be attributed to the discrepancy between the tMCAO model and MMD in clinical settings, which is a chronic and progressive disease. We then used the hind-limb ischemia model by femoral artery ligation as an established model of chronic ischemia, which is known to be an animal model

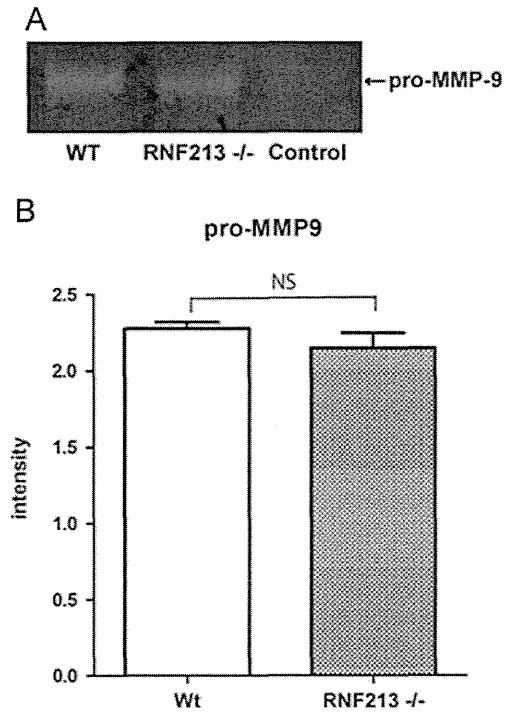

Fig. 7 – pro-MMP-9 expression in the GC muscle 24 h after tMCAO. (A) Representative photographs of gelatin zymography in Wt, RNF213-/-, and control specimens from the non-ischemic limbs of Wt. pro-MMP-9 was detected as 105 kDa. MMP-9 was not detected. (B) Semi-quantitative analysis of pro-MMP-9 expression. No significant difference was observed between Wt and RNF213-/-. (NS, not significant).

ideal for mimicking human occlusive artery disease and investigating angiogenesis (Limbourg et al., 2009). In this model, angiogenesis and blood flow recovery after femoral artery ligation were both significantly better in RNF213-/- than in Wt. Furthermore, ambulatory impairments in the ischemic hind-limb were significantly milder in RNF213 -/- than in Wt three and seven days after ligation.

Regarding *in vitro* culture studies, Kim and colleagues reported that tube formation by circulating endothelial progenitor cells (EPCs) from MMD patients was less in an *in vitro* assay of angiogenic activity (Kim et al., 2010). Hitomi and colleagues demonstrated that tube formation in induced pluripotent stem cells (iPSCs) derived from the vascular endothelial cells of MMD patients was less *in vitro* (2013). They also showed that the overexpression of RNF213 R4810K alleles inhibited the proliferation of human umbilical vein endothelial cells (HUVECs) (Hitomi et al., 2013). These findings were inconsistent with the results of the present study because we found that the target disruption of *RNF213* in mice resulted in enhanced angiogenesis *in vivo* under ischemic conditions. The following reasons may explain the conflicting results observed between ours and previous *in vitro* studies. Firstly, we used an *in vivo* model under the pathological condition of ischemia; thus, various biological backgrounds including immune responses mediated by blood cells should have participated in our system. RNF213 is known to be markedly expressed in blood cells and the spleen, which again suggested the contribution of the immune system in the present study (Kamada et al., 2011). Furthermore, the discrepancy between the angiogenic assay *in vitro* and that *in vivo* was suggested by Hitomi and colleagues (2013). Interactions between endothelial cells (ECs) and vascular smooth muscle cells (VSMCs) (Milliat et al., 2006), blood cells, and others are necessary for angiogenesis in the living body. Thus, our *in vivo* model is more likely to reflect pathophysiological angiogenesis in patients with MMD.

To further clarify the mechanism underlying enhanced angiogenesis after chronic ischemia in RNF213 -/-, we compared the expression of the extracellular matrix protein, MMP-9 between RNF213 -/- and Wt because the expression of MMP-9 was previously shown to be increased in patients with MMD (Fujimura et al., 2009; Kang et al., 2010), and MMP-9 is also known to participate in angiogenesis under various pathophysiological conditions (Kaczmarek, 2013; Lei et al., 2013). Furthermore, MMP-9 is attracting attention because it could be a therapeutic target during the postoperative period; elevated MMP-9 levels in the acute phase after revascularization surgery have been suggested to affect blood brain barrier impermeability, subsequently leading to cerebral hyperperfusion as a surgical complication (Fujimura et al., 2014). In the present study, no significant difference was observed in the expression of MMP-9 under ischemic conditions between RNF213 -/- and Wt; therefore, it is conceivable that enhanced angiogenesis in RNF213-/- could be mediated by an MMP-9-independent pathway. A further evaluation of other angiogenic factors including vascular endothelial growth factors and its receptors is necessary to answer this critical question. Alternatively, we cannot rule out the possibility that the increased expression of MMP-9 in blood cells may affect angiogenic responses in RNF213 -/-, and a further evaluation including the immune system in RNF213-/- may identify the underlying mechanisms for enhanced angiogenesis in mice lacking *RNF213*, a susceptibility gene for MMD.

4. Conclusion

Angiogenesis was enhanced in mice lacking *RNF213* after chronic hind-limb ischemia, which suggested the potential role of the *RNF213* gene abnormality in the development of abnormal vascular networks in chronic ischemia.

5. Experimental procedures

5.1. *Generation of RNF213 knockout mice*

We generated *RNF213* knockout mice by deleting exon 32 of *RNF213* with the Cre/loxP system as previously described (Kamada et al., 2011). Heterozygous male and female mice were bred to produce homozygous offspring (RNF213 -/-). Genotyping was performed by PCR using specific primers to exon 32 (Kamada et al., 2011).

5.2. *Experimental animals*

Male RNF213 -/- and wild-type littermates (Wt) were used in accordance with the National Institute of Health Guide for the Care and Use of Laboratory Animals (NIH Publications No. 80-23, revised 1996). All procedures were approved by the animal care facility of Tohoku University Graduate School of Medicine.

5.3. *Focal cerebral ischemia*

Eight- to ten-week-old male RNF213 -/- and Wt. were subjected to transient middle cerebral artery occlusion (tMCAO) by the intraluminal suture technique. Mice were anesthetized with 1.3 to 1.5% isofluorane in 30% oxygen and 70% nitrous oxide and breathed spontaneously. Rectal temperature during all surgical procedures was maintained at 37±0.5 °C using a feedback-regulated heating pad (BWT- 100, Bio Research Center, Nagoya, Japan). The mouse was placed a supine position, the neck was incised at the midline between the manubrium and the jaw, and the left common carotid artery (CCA) was carefully separated from the vagus nerve. The superior thyroid artery was cauterized and cut. The external carotid artery (ECA) was ligated with a 7-0 nylon suture near its bifurcation into the lingual and maxillary arteries and cauterized distally to the suture. The occipital artery was cauterized and cut. The pterygopalatine artery was then exposed and isolated. A collar suture at the origin of the ECA was prepared using a 6-0 silk suture, the ICA was closed using a vascular clip (MH-1–20, BEAR Medic, Tokyo, Japan), and the CCA was temporarily ligated with a 7-0 nylon suture. A silicon-coated 6-0 nylon monofilament (602323PK5Re, Doccol, Redlands, CA, USA) was introduced into the arteriotomy hole in the ECA and was advanced into the CCA bifurcation. After removing the vascular clip and cutting the ECA, the suture was advanced distally into the ICA. Once the tip of the inserted suture reached the ICA, the collar suture of the ECA was tightened to avoid bleeding from the arteriotomy hole, and the suture of the CCA was unfastened to restore blood flow from the CCA. The intraluminal suture was inserted into the ICA 9.0±0.5 mm from the CCA bifurcation until mild resistance was felt. The collar suture of the ECA stump was tightened securely around the inserted filament. The wound was closed with 6-0 nylon sutures, and the intraluminal suture was hidden in the wound. The mouse was then placed in a prone position and fixed in a head holder (SG-4 N, Narishige, Tokyo, Japan). Its scalp was shaved and cut with surgical scissors to expose the thin skull over the bilateral cerebral and cerebellar hemispheres. The surface of the skull was covered with a slipcover over a thin layer of saline to prevent drying. We recorded cerebral blood flow (CBF) values through the intact skull for 20 s using laser speckle flowmetry (LSF) (OMEGAZONE, Omegawave, Tokyo, Japan) and confirmed decreases in the CBF value in the MCA territory. The mouse was then allowed to regain consciousness. The mouse was re-anesthetized and fixed in the head holder in a prone position, and the CBF value was recorded. Mice in which CBF values were spontaneously restored were excluded from further experiments. The mouse was then placed again in a supine position and the cervical wound was reopened. The intraluminal suture was withdrawn gently and slowly to achieve reperfusion 90 min after the induction of ischemia and the ECA was ligated with the collar suture. The mouse was awakened to allow for a survival period.

5.4. *Infarction volume after tMCAO*

The infarction volume after tMCAO was measured in 14 mice (Wt, $n=7$; RNF213 -/-, $n=7$). Mice were given an overdose of isoflurane 48 h after 90 min MCAO, and then subjected to the transcardiac perfusion of cold saline. Brains were removed immediately and cut into 5 serial 2-mm-thick coronal sections. These sections were incubated in 1% solution of 2, 3, 5-triphenyltetrazolium chloride (TTC) (17779-10XX10MLML-FF, Sigma-Aldrich, St Louis, Mo, USA) for 10 min at 37 °C. Images were captured using a digital camera (GR DIGITAL III, 173240, Ricoh, Tokyo, Japan). Unstained areas were measured on TTC-stained sections as the infarct volume by Image J, version 1.46r (National Institutes of Health).

5.5. *Brain water content after tMCAO*

Brain water content was examined to assess the extent of cerebral edema after tMCAO. Ten mice were evaluated (Wt, $n=5$; RNF213-/-, $n=5$). Water content in each hemisphere was measured by the dry-wet method as previously described (Naruse et al., 1991). Mice were given an overdose of isoflurane 24 h after 90 min MCAO, and the brains were removed immediately. The hemispheres were weighed to obtain the wet and dry weights before and after drying at 100 °C for 48 h. Brain water content was calculated as 100% × (wet weight - dry weight) / wet weight.

5.6. *Evaluation of angiogenesis by immunohistochemical analysis of CD31*

Mice surviving until 28 days after 90 min MCAO were given an overdose of isoflurane and subjected to the transcardiac perfusion of cold saline followed by 4% paraformaldehyde (PFA). After fixation, the brain was removed and embedded in O.C.T. compound (Tissue-Tek, Sakura Finetek Japan, Tokyo, Japan), and then frozen. Sections were cut in the coronal plane at a thickness of 7 μm using a cryostat (Tissue-Tek Cryo3, Sakura Finetek Japan, Tokyo, Japan). The capillaries were visualized by immunofluorescent staining with an anti-CD31 antibody (Purified anti-mouse CD31 antibody, catalog no. 102501, BioLegend, CA USA), which stained endothelial cells. The sections were blocked with 10% bovine serum albumin (BSA) and 0.2% Triton X-100 (catalog no. X100-500 ML, Sigma-Aldrich, MO, USA) for 30 min at room temperature, and then incubated with the anti-CD31 antibody (1:100) overnight at 4 °C. The sections were then washed with PBS and incubated with secondary biotinylated anti-rat IgG (Biotinylated Anti-Rat IgG Antibody, catalog no. BA-4000, Vector Labs, CA, USA) for 30 min, followed by washing in phosphate buffered saline (PBS) and incubation with the VECTASTAIN Elite ABC Kit (Standard) (catalog no. PK-6100, Vector Labs, CA, USA). The signal was developed with Diaminobenzidine (DAB) (catalog no. 347-00904, DOJINDO, Kumamoto, Japan) and counterstained with hematoxylin.

The number of capillaries was counted in three random representative high power fields at 400x to obtain average values.

5.7. *Gelatin zymography after MCAO*

Gelatin zymography was performed on samples from ischemic hemispheres to evaluate the level of pro-matrix metalloproteinase (MMP)-9 and MMP-9 24 h after 90 min MCAO. Mice (Wt, $n=4$; RNF213 -/-, $n=3$) were given an overdose of isoflurane and subjected to the transcardiac perfusion of cold saline 24 h after reperfusion. Both hemispheres were rapidly removed and homogenized on ice in 1 ml of lysis buffer containing 50 mM Tris–HCl, pH 7.6, 150 mM NaCl, 5 mM $CaCl_2$, 0.05% BRIJ-35, 0.02% NaN_3, and 1% Triton-X-100. Homogenates were centrifuged at 10,000 g for 10 min at 4 °C. To analyze the MMP-9 level, protein was extracted from the tissue as previously described (Fujimura et al., 1999). The supernatants were recovered and incubated with gelatin-sepharose 4B (17-0956-01, GE Healthcare, Uppsala, Sweden) for 60 min with constant shaking at 4 °C. After incubation, the samples were centrifuged at 500 g for 2 min. The pellets were washed with a buffer containing 50 mM Tris–HCl, pH 7.6, 150 mM NaCl, 5 mM $CaCl_2$, 0.05% BRIJ-35 and 0.02% NaN_3. After a second centrifugation, the pellets were resuspended in elution buffer (50 mM Tris–HCl, pH 7.6, 150 mM NaCl, 5 mM $CaCl_2$, 0.05% BRIJ-35, 0.02% NaN_3, 10% dimethylsulfoxide) for 30 min. The samples were subjected to gelatin zymography with a Gelatin Zymo-Electrophoresis Kit (AK47, Primary Cell, Hokkaido, Japan) according to the manufacturer's directions. Images were captured and analyzed by the ChemiDoc MP ImageLab PC system (BioRad, CA, USA). The relative intensities of individual intensities were normalized by the value in a control sample. A non-ischemic hemisphere was adopted as the control.

5.8. *Hind-limb ischemia model*

Ten- to twelve-week-old male Wt and RNF213 -/- were used. Fourteen mice were subjected to this model (Wt, $n=7$; RNF213 -/-, $n=7$). The hind-limb ischemia model was created as previously described (Couffinhal et al., 1998; Limbourg et al., 2009; Lu et al., 2012). Mice were anesthetized with 1.3 to 1.5% isofluorane in 30% oxygen and 70% nitrous oxide and breathed spontaneously. Rectal temperature during all surgical procedures was maintained at 37 ± 0.5 °C using a feedback-regulated heating pad (BWT-100, Bio Research Center, Nagoya, Japan). After a 5-mm skin incision in the inguinal region on the left side, the femoral artery was blunt dissected and separated from the femoral vein and nerve. The femoral artery was tightly ligated distal to the origin of the deep branch with a 7-0 nylon suture and ischemia was induced in the hind-limb. The skin incision was closed by a 6-0 nylon suture. The mouse was then allowed to regain consciousness.

5.9. *Blood flow analysis in the hind-limbs*

Blood flow values in the both legs were recorded for 20 s using laser speckle flowmetry (LSF) (OMEGAZONE, Omegawave, Tokyo, Japan) before, immediately after ligation of the femoral artery, and at the different time points of postoperative days 3, 7, 14, 21, and 28. Since penetration of the laser beam was low, the majority of signals reflected skin perfusion depending on blood flow in the femoral artery. During measurements, mice were placed on a heat pad, kept at 37 °C, anesthetized with 1.3 to 1.5% isofluorane in 30% oxygen and 70% nitrous oxide, and breathed spontaneously.

5.10. *Ambulatory impairment scoring*

The severity of ambulatory impairments was assessed before ligation of the femoral artery and at the different time points of postoperative days 3, 7, 14, 21, and 28. The severity of ambulatory impairments was evaluated using the following scoring as described previously (Fig. 5A): 0, normal response (plantar/toe flexion in response to tail traction); 1, plantar, but not toe flexion; 2, no plantar or toe flexion; 3, dragging of the foot; 4, spontaneous movement of the non-ischemic hind-limb (Bosch-Marce et al., 2007; Lu et al., 2012).

5.11. *Immunohistochemistry analysis of the gastrocnemius muscle*

Twenty-eight days after ligation of the femoral artery, all mice which were subjected to hind-limb ischemia model were euthanized, and left gastrocnemicus (GC) muscle of each animal was removed. Frozen sections were made in the similar procedures as the brain. The sections were stained immunofluorescently anti-CD31 (Purified anti-mouse CD31 Antibody, catalog no. 102501, BioLegend, CA USA), anti-CD34 (anti-CD34 antibody, catalog no. ab8158, abcam, Massachusetts, UK) and anti-CD133 (Anti-Mouse CD133 Purified, eBioscience, catalog no. 14-1331-80, CA, USA) antibodies in the similar procedures as the brain with a little modification. Briefly, the sections had to be heated in the antigen retrieval buffer (Histo VT One, catalog no. 06380, Nacalai Tesque, Kyoto, Japan) before blocking with 10% BSA. Other procedures were same as described above.

5.12. *Gelatin zymography of the gastrocnemius muscle*

Gelatin zymography was performed on samples from the ischemic GC muscle to evaluate the level of MMP-9 three days after ligation of the femoral artery. Eight mice (Wt, $n=4$; RNF213 -/-, $n=4$) were euthanized three days after ligation of the femoral artery and both GC muscles were rapidly removed. The extraction of matrix metalloproteinases and gelatin zymography were performed using the same procedures as described above. The relative intensity of an individual sample was normalized by the value obtained in a control sample. The non-ischemic limb was adopted as the control.

5.13. *Statistical analysis*

All values were given as the mean$\pm$SD. Significance was assessed with a repeated measures two-way ANOVA and subsequent Bonferroni post hoc test for the blood flow analysis. A repeated measures two-way ANOVA and subsequent Mann-Whitney post hoc test were used to analyze

ambulatory impairments. The Student's t-test was used to analyze the infarct volume, brain water content, immunohistochemistry of CD31, and gelatin zymography. Values of $p<0.05$ were considered significant. Graph Pad Prism 5.03 (Graph Pad Software, La Jolla, CA, USA) was used for all statistical analysis.

Disclosure of funding

This study was supported by JSPS KAKENHI Grant Number 24659642.

Acknowledgment

This study was supported by JSPS KAKENHI Grant Number 24659642.

REFERENCES

Achrol, A.S., Guzman, R., Lee, M., Steinberg, G.K., 2009. Pathophysiology and genetic factors in moyamoya disease. Neurosurg. Focus 26, E4.

Bosch-Marce, M., Okuyama, H., Wesley, J.B., Sarkar, K., Kimura, H., Liu, Y.V., 2007. Effects of aging and hypoxia-inducible factor-1 activity on angiogenic cell mobilization and recovery of perfusion after limb ischemia. Circ. Res. 101, 1310–1318.

Couffinhal, T., Silver, M., Zheng, P.L., Kearney, M., Witzenbichler, B., Isner, M.J., 1998. Mouse model of angiogenesis. Am. J. Pathol. 152, 1667–1679.

Endo, M., Kawano, N., Miyaska, Y., Yada, K., 1989. Cranial burr hole for revascularization in moyamoya disease. J. Neurosurg. 71, 180–185.

Fujimura, M., Gasche, Y., Morita-Fujimura, Y., Massengale, J., Kawase, M., Chan, P.H., 1999. Early appearance of activated matrix metalloproteinase-9 and blood–brain barrier disruption in mice after focal cerebral ischemia and reperfusion. Brain Res. 842, 92–100.

Fujimura, M., Watanabe, M., Narisawa, A., Shimizu,, H., Tominaga, T., 2009. Increased expression of serum Matrix Metalloproteinase-9 in patients with moyamoya disease. Surg. Neurol. 72, 476–480.

Fujimura, M., Niizuma, K., Inoue, T., Sato, K., Endo, H., Shimizu, H., Tominaga, T., 2014. Minocycline prevents focal neurological deterioration due to cerebral hyperperfusion after extracranial-intracranial bypass for moyamoya disease. Neurosurgery 74, 163–170.

Hitomi, T., Habu, T., Kobayashi, H., Okuda, H., Harada, K.H., Osafune, K., Taura, D., Sone, M., Asaka, I., Ameku, T., Watanabe, A., Kasahara, T., Sudo, T., Shiota, F., Hashikata, H., Takagi, Y., Morito, D., Miyamoto, S., Nakao, K., Koizumi, A., 2013. Downregulation of securin by the variant RNF213 R4810K (rs112735431, G>A) reduces angiogenic activity of induced pluripotent stem cell-derived vascular endothelial cells from moyamoya patients. Biochem. Bioph. Res. Co. 438, 13–19.

Ikeda, H., Sasaki, T., Yoshimoto, T., Fukui, M., Arinami, T., 1999. Mapping of a familial moyamoya disease gene to chromosome 3p24.2-p26. Am. J. Hum. Genet. 64, 533–537.

Inoue, T.K., Ikezaki, K., Sasazuki, T., Matsushima, T., Fukui, M., 2000. Linkage analysis of moyamoya disease on chromosome 6. J. Child Neurol. 15, 179–182.

Kaczmarek, L., 2013. Mmp-9 inhibitors in the brain: can old bullets shoot new targets?. Curr. Pharm. Design 19, 1085–1089.

Kaku, Y., Morioka, M., Ohmori, Y., Kawano, T., Kai, Y., Fukuoka, H., Hirai, T., Yamashita, Y., Kuratsu, J., 2012. Outer-diameter narrowing of the internal carotid and middle cerebral arteries in moyamoya disease detected on 3D constructive interference in steady-state MR image: is arterial constrictive remodeling a major pathogenesis?. Acta Neurochir. (Wien) 154, 2151–2157.

Kamada, F., Aoki, Y., Narisawa, A., Abe, Y., Komatsuzaki, S., Kikuchi, A., Kanno, J., Niihori, T., Ono, M., Ishii, N., Owada, Y., Fujimura, M., Mashimo, Y., Suzuki, Y., Hata, A., Tsuchiya, S., Tominaga, T., Matsubara, Y., Kure, S., 2011. A genome-wide association study identifies RNF213 as the first Moyamoya disease gene. J. Hum. Genet. 56, 34–40.

Kang, H.S., Kim, J.H., Phi, J.H., Kim, Y.Y., Kim, J.E., Wang, K.C., Cho, B.K., Kim, S.K., 2010. Plasma matrix metalloproteinases, cytokines and angiogenic factors in moyamoya disease. J. Neurol. Neurosur. Ps.. 81, 673–678.

Kim, S.J., Heo, K.G., Shin, H.Y., Bang, O.Y., Kim, G.M., Chung, C.S., Kim, K.H., Jeon, P., Kim, J.S., Hong, S.C., Lee, K.H., 2010. Association of thyroid autoantibodies with moyamoya-type cerebrovascular disease: a prospective study. Stroke 41, 173–176.

Lei, C., Lin, S., Zhang, C., Tao, W., Dong, W., Hao, Z., 2013. Activation of cerebral recovery by matrix metalloproteinase-9 after intracerebral hemorrhage. Neuroscience 230, 86–93.

Limbourg, A., Korff, T., Napp, L.C., Schaper, W., Drexler, H., Limbourg, F.P., 2009. Evaluation of postnatal arteriogenesis and angiogenesis in a mouse model of hind-limb ischemia. Nat. Protocol 4, 1737–1746.

Liu, W., Morito, D., Takashima, S., Mineharu, Y., Kobayashi, H., Hitomi, T., Hashikata, H., Matsuura, N., Yamazaki, S., Toyoda, A., Kikuta, K., Takagi, Y., Harada, K.H., Fujiyama, A., Herzig, R., Krischek, B., Zou, L., Kim, J.E., Kitakaze, M., Miyamoto, S., Nagata, K., Hashimoto, N., Koizumi, A., 2011. Identification of RNF213 as a susceptibility gene for moyamoya disease and its possible role in vascular development. PLoS One 6, e22542.

Lu, Q., Yao, Y., Yao, Y., Liu, S., Huang, Y., Lu, S., 2012. Angiogenic factor AGGF1 promotes therapeutic angiogenesis in a mouse limb ischemia model. PloS One 7, e46998.

Matsushima, T., Fujiwara, S., Nagata, S., Fujii, K., Fukui, M., Kitamura, K., 1989. Surgical treatment for paediatric patients with moyamoya disease by indirect revascularization procedures (EDAS, EMS, EMAS). Acta Neurochir. (Wien) 98, 135–140.

Matsushima, T., Inoue, T., Suzuki, S.O., Fujii, K., Fukui, M., Hasuo, K., 1992. Surgical treatment of moyamoya disease in pediatric patients–comparison between the results of indirect and direct revascularization procedures. Neurosurgery 31, 401–405.

Milliat, F., Francois, A., Isoir, M., Deutsch, E., Tamarat, R., Tarlet, G., 2006. Influence of endothelial cells on vascular smooth muscle cells phenotype after irradiation: implication in radiation-induced vascular damages. Am. J. Pathol. 169, 1484–1495.

Miyawaki, S., Imai, H., Shimizu, M., Yagi, S., Ono, H., Mukasa, A., Nakatomi, H., Shimizu, T., Saito, N., 2013. Genetic variant RNF213 c.14576 G>A in various phenotypes of intracranial major artery stenosis/occlusion. Stroke 44, 2894–2897.

Murakami, K., Kondo, T., Kawase, M., Chan, P.H., 1998. The development of a new mouse model of global ischemia: focus on the relationships between ischemia duration, anesthesia, cerebral vasculature, and neuronal injury following global ischemia in mice. Brain Res. 780, 304–310.

Naruse, S., Aoki, Y., Takei, R., Horikawa, Y., Ueda, S., 1991. Effects of atrial natriuretic peptide on ischemic brain edema in rats evaluated by proton magnetic resonance method. Stroke 22, 61–65.

Oka, K., Yamashita, M., Sadoshima, S., Tanaka, K., 1981. Cerebral haemorrhage in Moyamoya disease at autopsy. Virchows Arch. A. 392, 247–261.

Research Committee on the Pathology and Treatment of Spontaneous Occlusion of the Circle of Willis, 2012. Health labour sciences research grant for research on measures for infractable diseases. guidelines for diagnosis and treatment of moyamoya disease (spontaneous occlusion of the circle of willis). Neurol. Med.-Chir. (Tokyo) 52, 245–266.

Sakurai, K., Horiuchi, Y., Ikeda, H., Ikezaki, K., Yoshimoto, T., Fukui, M., Arinami, T., 2004. A novel susceptibility locus for moyamoya disease on chromosome 8q23. J. Hum. Genet. 49, 278–281.

Sonobe, S., Fujimura, M., Niizuma, K., Nishijima, Y., Ito, A., Shimizu, H., Kikuchi, A., Arai-Ichioi, N., Kure, S., Tominaga, T., 2014. Temporal profile of the vascular anatomy evaluated by 9.4- T magnetic resonance angiography and histopathological analysis in mice lacking RNF213: A susceptibility gene for moyamoya disease. Brain Res. 1552, 64–71.

Suzuki, J., Takaku, A., 1969. Cerebrovascular "moyamoya" disease. Disease showing abnormal net-like vessels in base of brain. Arch. Neurol. 20, 288–299.

Takagi, Y., Kikuta, K., Nozaki, K., Hashimoto, N., 2007b. Histological features of middle cerebral arteries from patients treated for Moyamoya disease. Neurol. Med.-Chir. (Tokyo) 47, 1–4.

Tashiro, Y., Nishida, C., Sato-Kusubata, K., Ohki-Koizumi, M., Ishihara, M., Sato, A., 2012. Inhibition of PAI-1 induces neutrophil-driven neoangiogenesis and promotes tissue regeneration via production of angiocrine factors in mice. Blood 119, 6382–6393.

Wu, Z., Jiang, H., Zhang, L., Xu, X., Zhang, X., Kang, Z., Song, D., Zhang, J., Guan, M., Gu, Y., 2012. Molecular analysis of RNF213 gene for moyamoya disease in the Chinese Han population. PLoS One 7, e48179.

Yamauchi, T., Tada, M., Houkin, K., Tanaka, T., Nakamura, Y., Kuroda, S., Abe, H., Inoue, T., Ikezaki, K., Matsushima, T., Fukui, M., 2000. Linkage of familial moyamoya disease (spontaneous occlusion of the circle of Willis) to chromosome 17q25. Stroke 31, 930–935.

Yang, G., Kitagawa, K., Matsushita, K., Mabuchi, T., Yagita, Y., Yanagihara, T., Matsumoto, M., 1997. C57BL/6 strain is most susceptible to cerebral ischemia following bilateral common carotid occlusion among seven mouse strains: selective neuronal death in the murine transient forebrain ischemia. Brain Res. 752, 209–218.

Yoshihara, T., Taguchi, A., Matsuyama, T., Shimizu, Y., Kikuchi-Taura, A., Soma, T., 2008. Increase in circulating CD34-positive cells in patients with angiographic evidence of moyamoya-like vessels. J. Cerebr. Blood F. Met. 28, 1086–1089.

Zhang, Z.G., Zhang, L., Jiang, Q., Zhang, R., Davies, K., Powers, C., 2000. VEGF enhances angiogenesis and promotes blood-brain barrier leakage in the ischemic brain. J. Clin. Invest. 106, 829–838.

REVIEW ARTICLE doi: 10.2176/nmc.ra.2014-0326

Neurol Med Chir (Tokyo) 55, 199–203, 2015 Online February 20, 2015

Cognitive Dysfunction Survey of the Japanese Patients with Moyamoya Disease (COSMO-JAPAN Study): Study Protocol

Yasushi TAKAGI,[1] Susumu MIYAMOTO;[1] COSMO-Japan Study Group

[1]*Department of Neurosurgery, Kyoto University Graduate School of Medicine, Kyoto, Kyoto*

Abstract

Moyamoya disease is a cerebrovascular occlusive disease characterized by progressive stenosis or by occlusion at the terminal portion of the bilateral internal carotid arteries. The unusual vascular network (moyamoya vessels) at the base of the brain with this disease as collateral channels is developed in this disease. Social independence because of cognitive impairment has recently been recognized as an important unsolved social issue with adult moyamoya disease. The patients with cognitive impairment have difficulty in proving their status because the standard neuroradiological and neuropsychological methods to define cognitive impairment with moyamoya disease are not determined. These patients with cognitive impairment should be supported by social welfare as psychologically handicapped persons. Thus Cognitive Dysfunction Survey of the Japanese Patients with Moyamoya Disease (COSMO-JAPAN study) is planned. In this study, we want to establish a standard finding of the cognitive impairment in patients with moyamoya disease.

Key words: moyamoya disease, cognitive dysfunction, [^{123}I]iomazenil-single photon emission computed tomography, neuropsychological study

Introduction

Moyamoya disease is a cerebrovascular occlusive disease characterized by progressive stenosis or by occlusion at the distal ends of bilateral internal carotid arteries.[1)] The unusual vascular network (moyamoya vessels) at the base of the brain of individuals with this disease is considered to represent collateral channels formed as a result of progressive brain ischemic changes.[1–3)] The etiology of the disease is undefined. The findings that the incidence of the disease is highest in East Asian people and that the condition is frequently familial, suggest the involvement of a genetic factor in its pathogenesis.[1)] Extracranial-intracranial bypass surgery has been established as an effective neurosurgical intervention that increases cerebral blood flow (CBF) and prevents from ischemic attacks.[4,5)] However, difficulty with social independence accompanied by cognitive impairment has recently been recognized as an important unsolved social issue faced by patients with adult moyamoya disease.[6–8)] These patients are physically independent in daily life, but economically dependent. It is very difficult for them to obtain vocational skills because of cognitive impairment. These patients with cognitive impairment should be supported by social welfare as psychologically handicapped persons. They have difficulty in proving their status because the standard neuroradiological and neuropsychological methods to define cognitive impairment with moyamoya disease are not determined. Generally, cognitive impairment has been described as a neuropsychological disorder occurring after strokes that shows as disturbances in memory, attention, performance, and social behavioral disturbances mainly in pediatric cases.[9,10)] However, recent reports have focused on adult cases with neurocognitive impairment even without neuroradiological evidence of major stroke.[8,11,12)] Nakagawara et al.[8)] indicated that even if infarction has not yet occurred, brain dysfunction was associated with persistent hemodynamic compromise in the medial frontal lobes that can be visualized using [^{123}I]iomazenil (IMZ)-single photon emission computed tomography (SPECT). This technique has the potential to become a tool for diagnosing cognitive impairment in adult moyamoya patients who do not show major abnormalities on computed

Received October 19, 2014; Accepted December 10, 2014

tomography (CT) scans or magnetic resonance imaging (MRI). In addition, a common methodology for neuropsychological evaluation of these patients is yet to be determined.[6,12,13] In this study, we want to establish the standard finding of the cognitive impairment in patients with moyamoya disease.

Materials and Methods

I. Methods/design

This is a prospective multicenter trial planning to analyze 60 patients with moyamoya disease. The study was approved by the Regional Ethical Review Board at Kyoto University (reference number: E-1754), and all patients will provide written informed consent before inclusion in the trial.

II. Inclusion and exclusion criteria

Inclusion criteria are as follows:

1. Male or female aged above 18 years under 60 years
2. Diagnosed as moyamoya disease or unilateral moyamoya disease on assessment by the neuroradiological committee[14]
3. Without intracranial hemorrhage including intracerebral hemorrhage, intraventricular hemorrhage, and subarachnoid hemorrhage
4. Without a large structural lesions (less than 1 cortical artery region) on neuroradiological studies
5. No neurological disorder influencing neuropsychological assessment, e.g., aphasia, hemianopsia, and agnosia
6. Modified Rankin scale ranging from 0 to 3
7. Without serious cognitive dysfunction assessed by subjective, objective symptoms, or daily life situation
8. Confirmation of informed consent

Exclusion criteria are as follows:

1. Quasi-moyamoya disease
2. Impossible to perform MRI
3. Assessment as unsuitable for this study

These criteria are also described in Table 1.

Table 1 Inclusion and exclusion criteria

Inclusion criteria
1. Male or female aged above 18 years under 60 years
2. Diagnosed as moyamoya disease or unilateral moyamoya disease on assessment by the neuroradiological committee
3. Without intracranial hemorrhage including intracerebral hemorrhage, intraventricular hemorrhage, and subarachnoid hemorrhage
4. Without a large structural lesions (less than 1 cortical artery region) on neuroradiological studies
5. No neurological disorder influencing neuropsychological assessment, e.g., aphasia, hemianopsia, and agnosia
6. Modified Rankin scale ranging from 0 to 3
7. Without serious cognitive dysfunction assessed by subjective, objective symptoms, or daily life situation
8. Confirmation of informed consent
Exclusion criteria
1. Quasi-moyamoya disease
2. Impossible to perform MRI
3. Assessment as unsuitable for this study

MRI: magnetic resonance imaging.

III. Background data

As background data of the patients, including in this study institute, sex, age, history of education, history of jobs, familial history, reason for diagnosis, modified Rankin scale, medication, and neurological deficits are recorded. In addition, blood sample is collected.

IV. SPECT

Brain N-isopropyl-p-^{123}I-iodoamphetamine (^{123}I-IMP) SPECT using QSPECT/dual table autoradiographic (ARG) method with three-dimensional stereotactic surface projection (3D-SSP) is performed to calculate the regional cerebral blood flow. To assess the regional cerebral vascular reserve, Diamox challenge SPECT is performed. The procedure for QSPECT/dual table ARG is described elsewhere in more detail.[15,16] The data is analyzed by the SEE-JET (stereotactic extraction estimation based on the Japan EC-IC bypass trial study) program.[17]

^{123}I-IMZ-SPECT using QSPECT method with 3D-SSP is performed to assess cortical neuronal loss. Cortical neuron loss is analyzed using the SEE method (level 3: gyrus level) for 3D-SSP Z-score maps as previously reported.[8]

V. MRI

MRI scans are also performed in all subjects. The scans are acquired on a 1.5 T or a 3 T scanner using a three-dimensional (3D) sagittal magnetization-prepared rapid gradient-echo imaging sequence, which is specially adjusted for the Japanese Alzheimer's disease Neuroimaging Initiative (J-ADNI) 1/2 protocols. T_1 structural sequences [3D MPRAGE on Siemens (Erlangen, Germany) and Philips Healthcare (Best, the Netherlands), 3D IR-SPGR on GE], FLAIR, T_2WI (Dual Echo), T_2*WI and TOF-MRA images are obtained in this study.[18]

VI. Neuropsychological assessment

Basic cognitive ability is evaluated using the

Table 2 Neuroradiological and neuropsychological study

Neuroradiological study
SPECT
^{123}I-IMP SPECT
^{123}I-IMZ-SPECT
MRI
MPRAGE/IR-SPGR
FLAIR
T_2WI (Dual Echo)
T_2*WI
TOF-MRA
Neuropsychological study
WAIS-III
WMS-R
FAB
WCST
Stroop test
Word-fluency
TMT A/B
BDI II
STAI
FrSBe
WHOQOL26

Wechsler Adult Intelligence Scale-Third Edition (WAIS-III) to assess intelligence, the Wechsler Memory Scale-Revised (WMS-R) to assess memory,[19,20] and supplemental subtests for each task. Several frontal-functioning tests are also administered to detect specific neuropsychological deficits associated with adult moyamoya disease that co-occurs with difficulty in social independence. The Frontal Assessment Battery (FAB) tests general frontal cognitive ability. The Trail Making Test Part A (TMT-A) assesses speed of information processing,[21,22] and the Trail Making Test Part B (TMT-B) and the Wisconsin Card Sorting Test (WCST) assess executive ability.[5,18] Stroop test, Word-fluency test, and Frontal Systems Behavior Scale (FrSBe) are also used for frontal lobe function.[22–24] The Beck Depression Inventory—Second Edition (BDI II) and State-Trait Anxiety Inventory (STAI) assess depressive state.[26,27] In addition, WHOQOL26 assesses the quality of life. The item of neuroradiological and neuropsychological study is summarized in Table 2.[28]

Discussion

Patients with moyamoya disease often suffer higher cognitive impairments such as memory, attention, and social behavioral disturbances.[11–13] Such cognitive impairments may occur in patients with medial frontal lobe damage including the anterior cingulate cortex. However, confirmatory diagnosis of higher cognitive dysfunction in patients with moyamoya disease without obvious brain damages on CT or MRI imaging has not been established and could become a social issue.[8]

In general, higher brain dysfunction associated with adult moyamoya disease could be detected by both neuropsychological findings and obvious medial frontal lobe damage detected by CT or MRI.[11–13] In addition, hemodynamic ischemia in this region is analyzed by SPECT at rest and after Diamox challenge.[15,16] More recently, loss of frontal cortical neuron could be estimated by functional neuroimaging using SPECT, because central benzodiazepine receptor mapping using ^{123}I-IMZ is available for clinical use.[8] IMZ is a specific radioactive tracer for the central benzodiazepine receptor that may be useful as a marker of cortical neuron loss. Recent work using IMZ-SPECT has demonstrated the association between cortical neuron loss in bilateral frontal medial cortices and cognitive dysfunction.[8]

Neuropsychological analysis in patients with brain damage played an important role in the history of developing the research of brain function.[13,19–22,29] Among brain dysfunction, higher cognitive dysfunction has been underestimated in the neurosurgical field. This dysfunction is often due to frontal lobe dysfunction. An extensive focus on frontal lobe function has not yet been taken by previous research regarding moyamoya disease. CBF and IMZ studies have shown that antero-medial frontal cortices fed by anterior circulation develop blood insufficiencies.[8,30] For this reason, several neuropsychological test batteries to evaluate frontal lobe functioning in relation to hemodynamic compromise were employed for our preliminary study. Based on this preliminary study, we developed this study and adopted several tasks to examine the frontal lobe functions.[11] To date, this is the first nation-wide survey of patients with moyamoya disease focusing on the neuroradiological and neuropsychological analysis in association with higher cognitive dysfunction. Patients with cognitive impairment should be supported by social welfare as psychologically handicapped persons.

The data obtained from the results of the study will play an important role in clarifying higher cognitive dysfunction in patients with moyamoya disease.

Conflicts of Interest Disclosure

All authors have no conflicts of interest in this manuscript.

References

1) Suzuki J, Kodama N: Moyamoya disease—a review. *Stroke* 14: 104–109, 1983
2) Hosoda Y, Ikeda E, Hirose S: Histopathological studies on spontaneous occlusion of the circle of Willis (cerebrovascular moyamoya disease). *Clin Neurol Neurosurg* 99(Suppl 2): S203–S208, 1997
3) Takekawa Y, Umezawa T, Ueno Y, Sawada T, Kobayashi M: Pathological and immunohistochemical findings of an autopsy case of adult moyamoya disease. *Neuropathology* 24: 236–242, 2004
4) Houkin K, Kuroda S, Ishikawa T, Abe H: Neovascularization (angiogenesis) after revascularization in moyamoya disease. Which technique is most useful for moyamoya disease? *Acta Neurochir (Wien)* 142: 269–276, 2000
5) Karasawa J, Kikuchi H, Furuse S, Kawamura J, Sakaki T: Treatment of moyamoya disease with STA-MCA anastomosis. *J Neurosurg* 49: 679–688, 1978
6) Festa JR, Schwarz LR, Pliskin N, Cullum CM, Lacritz L, Charbel FT, Mathews D, Starke RM, Connolly ES, Marshall RS, Lazar RM: Neurocognitive dysfunction in adult moyamoya disease. *J Neurol* 257: 806–815, 2010
7) Miyamoto S, Nagata I, Hashimoto N, Kikuchi H. Direct anastomotic bypass for cerebrovascular moyamoya disease. *Neurol Med Chir (Tokyo)* 38(Suppl): 294–296, 1998
8) Nakagawara J, Osato T, Kamiyama K, Honjo K, Sugio H, Fumoto K, Murahashi T, Takada H, Watanabe T, Nakamura H: Diagnostic imaging of higher brain dysfunction in patients with adult moyamoya disease using statistical imaging analysis for [123I]iomazenil single photon emission computed tomography. *Neurol Med Chir (Tokyo)* 52: 318–326, 2012
9) Matsushima Y, Aoyagi M, Masaoka H, Suzuki R, Ohno K: Mental outcome following encephaloduroarteriosynangiosis in children with moyamoya disease with the onset earlier than 5 years of age. *Childs Nerv Syst* 6: 440–443, 1990
10) Sato H, Sato N, Tamaki N, Matsumoto S: Chronic low-perfusion state in children with moyamoya disease following revascularization. *Childs Nerv Syst* 6: 166–171, 1990
11) Araki Y, Takagi Y, Ueda K, Ubukata S, Ishida J, Funaki T, Kikuchi T, Takahashi JC, Murai T, Miyamoto S: Cognitive function of patients with adult moyamoya disease. *J Stroke Cerebrovasc Dis* 23: 1789–1794, 2014
12) Karzmark P, Zeifert PD, Bell-Stephens TE, Steinberg GK, Dorfman LJ: Neurocognitive impairment in adults with moyamoya disease without stroke. *Neurosurgery* 70: 634–638, 2012
13) Weinberg DG, Rahme RJ, Aoun SG, Batjer HH, Bendok BR: Moyamoya disease: functional and neurocognitive outcomes in the pediatric and adult populations. *Neurosurg Focus* 30: E21, 2011
14) Research Committee on the Pathology and Treatment of Spontaneous Occlusion of the Circle of Willis; Health Labour Sciences Research Grant for Research on Measures for Infractable Diseases: Guidelines for diagnosis and treatment of moyamoya disease (spontaneous occlusion of the circle of Willis). *Neurol Med Chir (Tokyo)* 52: 245–266, 2012
15) Iida H, Nakagawara J, Hayashida K, Fukushima K, Watabe H, Koshino K, Zeniya T, Eberl S: Multicenter evaluation of a standardized protocol for rest and acetazolamide cerebral blood flow assessment using a quantitative SPECT reconstruction program and split-dose 123I-iodoamphetamine. *J Nucl Med* 51: 1624–1631, 2010
16) Yoneda H, Shirao S, Koizumi H, Oka F, Ishihara H, Ichiro K, Kitahara T, Iida H, Suzuki M: Reproducibility of cerebral blood flow assessment using a quantitative SPECT reconstruction program and split-dose 123I-iodoamphetamine in institutions with different γ-cameras and collimators. *J Cereb Blood Flow Metab* 32: 1757–1764, 2012
17) Mizumura S, Nakagawara J, Takahashi M, Kumita S, Cho K, Nakajo H, Toba M, Kumazaki T: Three-dimensional display in staging hemodynamic brain ischemia for JET study: objective evaluation using SEE analysis and 3D-SSP display. *Ann Nucl Med* 18: 13–21, 2004
18) Imabayashi E, Matsuda H, Tabira T, Arima K, Araki N, Ishii K, Yamashita F, Iwatsubo T; Japanese Alzheimer's Disease Neuroimaging Initiative: Comparison between brain CT and MRI for voxel-based morphometry of Alzheimer's disease. *Brain Behav* 3: 487–493, 2013
19) Wechsler D: *Wechsler Adult Intelligence Scale, ed 3.* San Antonio, The Psychological Corporation, 1997
20) Wechsler D: *Wechsler Memory Scale-Revised.* San Antonio, The Psychological Corporation, 1987
21) Dubois B, Slachevsky A, Litvan I, Pillon B: The FAB: a Frontal Assessment Battery at bedside. *Neurology* 55: 1621–1626, 2000
22) Yoon B, Shim YS, Cheong HK, Hong YJ, Lee KS, Park KH, Ahn KJ, Kim DJ, Kim YD, Choi SH, Yang DW: White matter hyperintensities in mild cognitive impairment: clinical impact of location and interaction with lacunes and medial temporal atrophy. *J Stroke Cerebrovasc Dis* 23: e365–e372, 2014
23) Reitan RM: *The Halstead-Reitan Neuropsychological Test Battery.* Tucson, Neuropsychology Press, 1985
24) Deckel AW, Hesselbrock V, Bauer L: Relationship between alcohol-related expectancies and anterior brain functioning in young men at risk for developing alcoholism. *Alcohol Clin Exp Res* 19: 476–481, 1995
25) Terada T, Obi T, Yoshizumi M, Murai T, Miyajima H, Mizoguchi K: Frontal lobe-mediated behavioral changes in amyotrophic lateral sclerosis: are they independent of physical disabilities? *J Neurol Sci* 309: 136–140, 2011
26) Takahashi M, Tanaka K, Miyaoka H: Depression and associated factors of informal caregivers versus professional caregivers of demented patients. *Psychiatry Clin Neurosci* 59: 473–480, 2005

27) Yamanishi T, Tachibana H, Oguru M, Matsui K, Toda K, Okuda B, Oka N: Anxiety and depression in patients with Parkinson's disease. *Intern Med* 52: 539–545, 2013
28) Matsuoka Y, Yoneda K, Sadahira C, Katsuura J, Moriue T, Kubota Y: Effects of skin care and makeup under instructions from dermatologists on the quality of life of female patients with acne vulgaris. *J Dermatol* 33: 745–752, 2006
29) Heaton RK, Chelune GJ, Talley JL, Kay GG, Curtis G: *Wisconsin Card Sorting Test (WCST) Manual, Revised and Expanded.* Odessa, FL, Psychological Assessment Resources, 1993
30) Kaku Y, Iihara K, Nakajima N, Kataoka H, Fukuda K, Masuoka J, Fukushima K, Iida H, Hashimoto N: Cerebral blood flow and metabolism of hyperperfusion after cerebral revascularization in patients with moyamoya disease. *J Cereb Blood Flow Metab* 32: 2066–2075, 2012

Appendix

I. COSMO-JAPAN study group

Kiyohiro Houkin, Department of Neurosurgery, Hokkaido University Graduate School of Medicine, Sapporo, Hokkaido, Japan

Joji Nakagawara, Integrative Stroke Imaging Center, Department of Neurosurgery, National Cerebral and Cardiovascular Center, Suita, Osaka, Japan

Kuniaki Ogasawara, Department of Neurosurgery, Iwate Medical University, Morioka, Iwate, Japan

Teiji Tominaga, Department of Neurosurgery, Tohoku University Graduate School of Medicine, Sendai, Miyagi, Japan

Yoshikazu Okada, Department of Neurosurgery, Tokyo Women's Medical University, Tokyo, Japan

Tadashi Nariai, Department of Neurosurgery, Graduate School, Tokyo Medical and Dental University School of Medicine, Tokyo, Japan

Satoshi Kuroda, Department of Neurosurgery, Graduate School of Medicine and Pharmaceutical Science, University of Toyama, Toyama, Toyama, Japan

Yukihiko Fujii, Department of Neurosurgery, Brain Research Institute, University of Niigata, Niigata, Niigata, Japan

Toshihiko Wakabayashi, Department of Neurosurgery, Nagoya University Graduate School of Medicine, Nagoya, Aichi, Japan

Kazuo Yamada, Department of Neurosurgery, Nagoya City University Graduate School of Medical Sciences, Nagoya, Aichi, Japan

Susumu Miyamoto, Department of Neurosurgery, Kyoto University Graduate School of Medicine, Kyoto, Kyoto, Japan

Hiroyuki Nakase, Department of Neurosurgery, Nara Medical University, Nara, Nara, Japan

Koji Iihara, Department of Neurosurgery, Graduate School of Medical Sciences, Kyushu University, Fukuoka, Fukuoka, Japan

Toshio Matsushima, Department of Neurosurgery, Faculty of Medicine, Saga University, Saga, Saga, Japan

Izumi Nagata, Department of Neurosurgery, Nagasaki University Graduate School of Biomedical Sciences, Nagasaki, Nagasaki, Japan

Toshiya Murai, Department of Psychiatry Graduate School of Medicine, Kyoto University, Kyoto, Kyoto, Japan

Tomohisa Okada, Department of Diagnostic Imaging and Nuclear Medicine, Kyoto University Graduate School of Medicine, Kyoto, Kyoto, Japan

Yasushi Takagi, Department of Neurosurgery, Kyoto University Graduate School of Medicine, Kyoto, Kyoto, Japan

II. Neuroradiological study committee

Joji Nakagawara, Integrative Stroke Imaging Center, Department of Neurosurgery, National Cerebral and Cardiovascular Center, Suita, Osaka, Japan

Tomohisa Okada, Department of Diagnostic Imaging and Nuclear Medicine, Kyoto University Graduate School of Medicine, Kyoto, Kyoto, Japan

III. Neuropsychological study committee

Toshiya Murai, Department of Psychiatry Graduate School of Medicine, Kyoto University, Kyoto, Kyoto, Japan

Takashi Nishikawa, Graduate School of Comprehensive Rehabilitation, Osaka Prefecture University, Habikino, Osaka, Japan

IV. Study protocol committee

Kuniaki Ogasawara, Department of Neurosurgery, Iwate Medical University, Morioka, Iwate, Japan

Toshio Matsushima, Department of Neurosurgery, Faculty of Medicine, Saga University, Saga, Saga, Japan

Yasushi Okada, Department of Cerebrovascular Medicine and Neurology, Clinical Research Institute, National Hospital Organization Kyushu Medical Center, Fukuoka, Fukuoka, Japan

Yasushi Takagi, Department of Neurosurgery, Kyoto University Graduate School of Medicine, Kyoto, Kyoto, Japan

Address reprint requests to: Yasushi Takagi, MD, PhD, Department of Neurosurgery, Kyoto University Graduate School of Medicine, Shogoin, Kawahara-cho, Sakyo-ku, Kyoto, Kyoto 606-8507, Japan.
e-mail: ytakagi@kuhp.kyoto-u.ac.jp

ORIGINAL ARTICLE doi: 10.2176/nmc.oa.2014-0360

Neurol Med Chir (Tokyo) 55, 204–209, 2015 Online February 20, 2015

Visualization of Periventricular Collaterals in Moyamoya Disease with Flow-sensitive Black-blood Magnetic Resonance Angiography: Preliminary Experience

Takeshi FUNAKI,[1] Yasutaka FUSHIMI,[2] Jun C. TAKAHASHI,[3] Yasushi TAKAGI,[1] Yoshio ARAKI,[4] Kazumichi YOSHIDA,[1] Takayuki KIKUCHI,[1] and Susumu MIYAMOTO[1]

Departments of [1]Neurosurgery and [2]Diagnostic Imaging and Nuclear Medicine, Kyoto University Graduate School of Medicine, Kyoto, Kyoto; [3]Department of Neurosurgery, National Cerebral and Cardiovascular Center, Suita, Osaka; [4]Department of Neurosurgery, Nagoya University Graduate School of Medicine, Nagoya, Aichi

Abstract

Fragile abnormal collaterals in moyamoya disease, known as "moyamoya vessels," have rarely been defined. While flow-sensitive black-blood magnetic resonance angiography (FSBB-MRA) is a promising technique for visualizing perforating arteries, as of this writing no other reports exist regarding its application to moyamoya disease. Six adults with moyamoya disease underwent FSBB-MRA. It depicted abnormal collaterals as extended lenticulostriate, thalamic perforating, or choroidal arteries, which were all connected to the medullary or insular artery in the periventricular area and supplied the cortex. This preliminary case series illustrates the potential for FSBB-MRA to reveal abnormal moyamoya vessels, which could be reasonably defined as periventricular collaterals.

Key words: moyamoya disease, periventricular anastomosis, black-blood magnetic resonance angiography

Introduction

Intracranial hemorrhage is a devastating symptom of moyamoya disease.[1)] Fragile abnormal vascular collaterals, known as "moyamoya vessels," are suspected as a source of bleeding.[1,2)] Although such collaterals are generally assumed to arise from dilated lenticulostriate arteries,[3,4)] the angiographical extension of dilated thalamic perforators or choroidal arteries is also known to involve bleeding.[5)] A pioneering study implied that all these types of collaterals arising from the lenticulostriate, thalamic perforating, and choroidal arteries clustered around the periventricular subependymal area to connect to the medullary arteries and were frequently associated with cerebral microbleeds.[6)] However, morphological details of the connection of such collaterals have not been sufficiently documented. Furthermore, because numerous overlapping vessels can obscure the view, angiography often fails to reveal these details.

Flow-sensitive black-blood magnetic resonance angiography (FSBB-MRA) is a recently introduced noninvasive black-blood imaging technique for visualizing perforating arteries.[7,8)] High-resolution 3-tesla FSBB-MRA can reveal tiny parenchymal arteries as well as cisternal and ventricular arteries in the coronal view of the brain. As of this writing, no previous report has addressed the use of FSBB-MRA in visualization of abnormal collateral vessels in moyamoya disease. Noninvasive detection of such collaterals might gain clinical significance in light of risk estimates of bleeding in moyamoya disease. In the present preliminary case series, this innovative imaging technique was applied to six patients with moyamoya disease to facilitate visualization and analysis of the morphological characteristics of periventricular collaterals.

Received October 14, 2014; Accepted November 26, 2014

Materials and Methods

I. Patients

Six adult patients (male 4, female 2) with moyamoya disease were included in the present study (Table 1). The age of these patients ranged from 34 years to 44 years. The mode of manifestation was intracranial hemorrhage in five patients and transient ischemic attack in one patient. All patients underwent magnetic resonance (MR) imaging including

Table 1 Summary of patients

Case	Age/Sex	Manifestation mode	Location of hemorrhage	Initial symptoms	Suzuki stage, R/L	Number of periventricular anastomoses (R/L)
1	43F	ICH	left temporal lobe	headache, speech disturbance	1/3	2 (1/1)
2	37M	ICH with IVH	right thalamus	headache, nausea	5/5	5 (3/2)
3	47M	ICH	left temporal lobe	hemiparesis, motor aphasia	4/4	3 (2/1)
4	37M	ICH	left insula and lateral part of thalamus	hemiparesis	0/3	3 (0/3)
5	34M	IVH	lateral ventricle	consciousness disturbance	5/5	5 (2/3)
6	44F	TIA	–	transient motor weakness	4/4	1 (1/0)

ICH: intracerebral hemorrhage, IVH: intraventricular hemorrhage, TIA: transient ischemic attack.

FSBB-MRA, routine clinical 3-tesla MR imaging including susceptibility-weighted imaging (SWI), and conventional cerebral angiography during the same admission period. All patients provided written informed consent to the FSBB-MRA.

II. Imaging technique

A 3-tesla research MR scanner (Vantage; Toshiba Medical Systems Corporation, Otawara, Tochigi) with a 32-channel head coil was used to obtain FSBB images. These images were scanned as coronal sections with the following parameters: repetition time (TR)/ echo time (TE), 35/13 ms; flip angle, 15°; acquisition matrix size, 384 × 384; and field of view (FOV), 192 × 192 mm in 1 axial 3D slab of 80 sections (0.8 mm thickness); and a parallel imaging factor of 2. The imaging field extended from the anterior horn to the atrium. A motion-probing gradient of b = 0.3 s/mm^2 was applied to dephase arterial blood flow in three directions. Total scan time was 8 m 31 s. In addition to source images with 0.8 mm thickness, minimum-intensity projection images were also generated as 2.5-mm thick and 10-mm thick slabs of overlapping volumes. Both minimum-intensity projection images and source images were assessed by a neuroradiologist and a neurosurgeon.

During the same admission period, all patients underwent MR imaging including FSBB-MRA, routine clinical 3-tesla MR imaging including susceptibility-weighted imaging (SWI) to detect the evidence of bleeding, and conventional cerebral angiography.

III. Analysis

Both a neurosurgeon (Takeshi Funaki) and a neuroradiologist (Yasutaka Fushimi) carefully compared the results of the arterial-phase angiography and FSBB-MRA for each patient. Periventricular anastomosis, the finding of interest in the present study, was defined as that between the perforating and medullary arteries or between the choroidal and medullary arteries, which was located around the periventricular area. Any topographical relationship between periventricular anastomoses and SWI-visible lesions was assessed on a workstation integrated into the image-archiving and communication system.

Results

Periventricular anastomoses were observed in FSBB-MRA images obtained from all six patients (Table 1). The morphologies of the periventricular anastomoses revealed in the FSBB-MRA images exactly coincided with those revealed in the arterial phase of angiography, confirming that FSBB-MRA truly depicted arteries. A total of 19 periventricular anastomoses were identified with FSBB-MRA. An SWI-visible lesion was identified at the exact sites of 11 anastomoses (57.9%).

Representative cases

Case 1: A 43-year-old female with moyamoya disease suffered from left temporal lobe hemorrhage. Left internal carotid artery angiography (Fig. 1a, b) revealed the medullary arteries derived from a lenticulostriate artery, suggesting an anastomosis between the lenticulostriate and medullary arteries around the periventricular area. FSBB-MRA more clearly revealed an anastomosis between these arteries at the lateral corner of the frontal horn of the ventricle with exact correspondence to angiography (Fig. 1c). Note that the medullary arteries have the largest caliber in the cortical area and smallest in their periventricular portion, indicating that the arteries originally arose from the cortical arteries. Blood flow was directed "ventriculofugally" toward

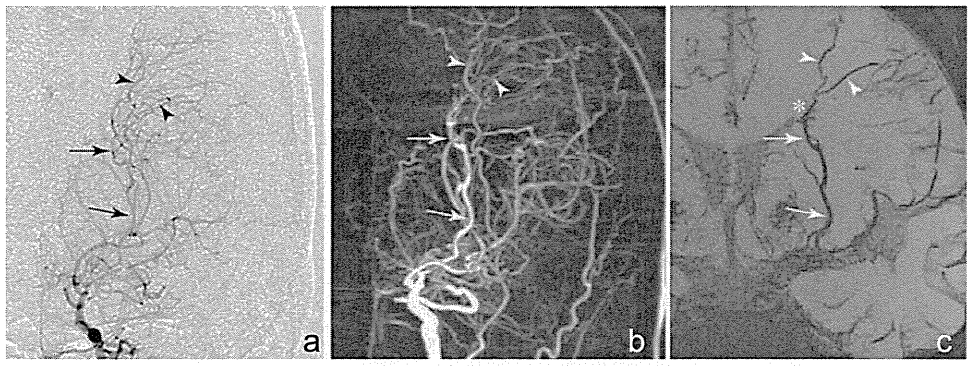

Fig. 1 Periventricular anastomosis originating from the lenticulostriate artery (Case 1). a: Anterior-posterior view of conventional angiography of the left internal carotid artery showing the medullary arteries (*arrowheads*) branching from a lenticulostriate artery (*arrows*). b: The same view of a maximum-intensity projection image reconstructed with 3-dimensional rotation angiography. c: Flow-sensitive black-blood magnetic resonance angiography revealing an anastomosis (*asterisk*) between the medullary arteries (*arrowheads*) and the lenticulostriate artery (*arrows*) at the lateral corner of the frontal horn of the ventricle.

the cortical area in the medullary arteries; it thus travels opposite to the original direction of flow in the medullary artery. In this patient, FSBB-MRA of the contralateral side revealed a very similar finding.

Case 2: A 37-year-old male with moyamoya disease suffered from right thalamic hemorrhage. Meticulous reading of left carotid artery angiography might identify a tortuous perforating artery originating from the thalamotuberal artery and connecting to the medullary arteries, but numerous overlapping vessels obscure the view (Fig. 2a). FSBB-MRA more clearly revealed the thalamotuberal artery, which coursed around the periventricular area of the third ventricle and then abnormally extended laterally beyond the thalamus and connected to the medullary artery (Fig. 2b). Note that a microbleed was revealed at the inflexion point of the collaterals, the site supposed to be the first anastomotic site, located beneath the ependymal layer of the third ventricle. In this patient, FSBB-MRA of the contralateral side revealed a very similar finding, where the evidence of thalamic hemorrhage was observed.

Case 3: A 47-year-old male with moyamoya disease suffered from left temporal lobe hemorrhage. Right vertebral artery angiography showed the probable thalamogeniculate artery connecting to the insular artery and subsequently to the middle cerebral artery, revealing a somewhat arbitrary spatial relationship (Fig. 3a). FSBB-MRA more clearly demonstrated the anastomosis between the thalamogeniculate artery and the insular artery, a type of medullary artery originally derived from the middle cerebral artery (Fig. 3b). The anastomosis was located at the inferolateral margin of the thalamus near the inferior horn of the lateral ventricle. SWI revealed a microbleed at the exact point of the anastomosis (Fig. 3c). In this patient, FSBB-MRA of the contralateral side revealed a similar finding, where the evidence of temporal lobe hemorrhage was observed.

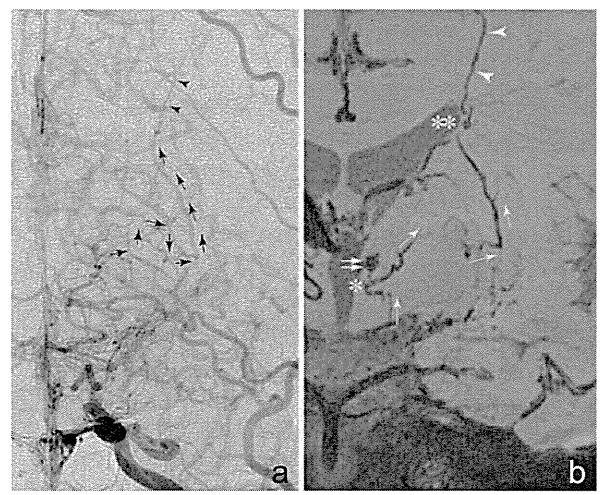

Fig. 2 Periventricular anastomosis originating from the thalamotuberal artery (Case 2). a: Anterior-posterior view of left common carotid artery angiography showing a tortuous thalamotuberal artery (*arrows*) connecting to the medullary arteries (*arrowheads*). b: Flow-sensitive black-blood magnetic resonance angiography demonstrating the arteries more clearly. Anastomotic sites are supposed to be located both beneath the ependyma of the third ventricle (*asterisk*) and at the lateral corner of the lateral ventricle (*double asterisk*). The evidence of bleeding is observed at the first anastomotic site (*double arrow*).

Case 4: A 37-year-old male with moyamoya disease suffered from hemorrhage extending through the lateral part of the thalamus and insula in the left

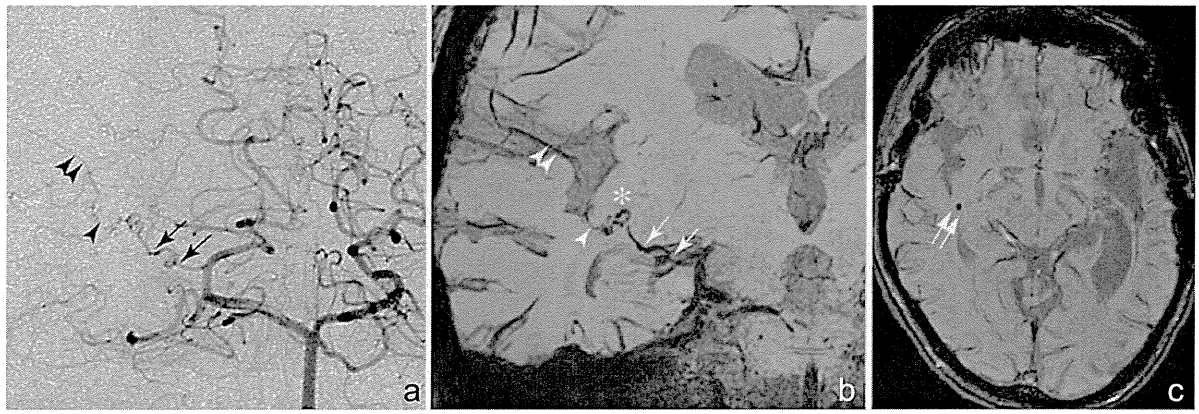

Fig. 3 Periventricular anastomosis originating in the thalamogeniculate artery (Case 3). a: Anterior-posterior view of vertebral artery angiography showing the thalamogeniculate artery (*arrows*), which connects to the insular artery (*arrowhead*) and subsequently to the middle cerebral artery (*double arrowhead*), revealing a somewhat arbitrary spatial relationship. b: Flow-sensitive black-blood magnetic resonance angiography more clearly demonstrating the anastomosis (*asterisk*) between the thalamogeniculate artery (*arrows*) and the insular artery (*arrowhead*), which is located at the temporal stem. c: Susceptibility-weighted imaging revealing a microbleed at the exact site of the anastomosis (*double arrow*).

hemisphere. Left internal carotid artery angiography showed an abnormal extension of the dilated choroidal artery (Fig. 4a, b). FSBB-MRA more clearly revealed anastomosis between the choroidal artery and the medullary artery beneath the lateral wall of the atrium of the lateral ventricle (Fig. 4c), with exact correspondence to the anterior-posterior view from the angiography. The evidence of a microbleed can be observed at the exact point of the anastomosis (Fig. 4c, d). In this patient, the anastomosis between the thalamogeniculate and insular arteries was also observed in the lateral part of the left thalamus, where the evidence of hematoma was observed.

Discussion

I. Periventricular anastomosis as a concept defining fragile collateral networks in moyamoya disease

In the present case series, all patients have a type of anastomosis between the perforating and medullary arteries or between the choroidal and medullary arteries. These types of anastomoses probably serve as a collateral to the cortex and compensate for the decrease in cerebral blood flow attributable to occlusion of the internal carotid artery. Such collaterals, although the subject of limited interest, have been denoted variously in previous reports as "anastomosis between the perforating branch and medullary artery,"[9] "abnormal vessel network/medullary artery anastomosis,"[4] or "lenticulostriate-medullary artery anastomosis."[3] Most of these collaterals, however, have barely been identified through meticulous angiographic observation and thus have rarely been

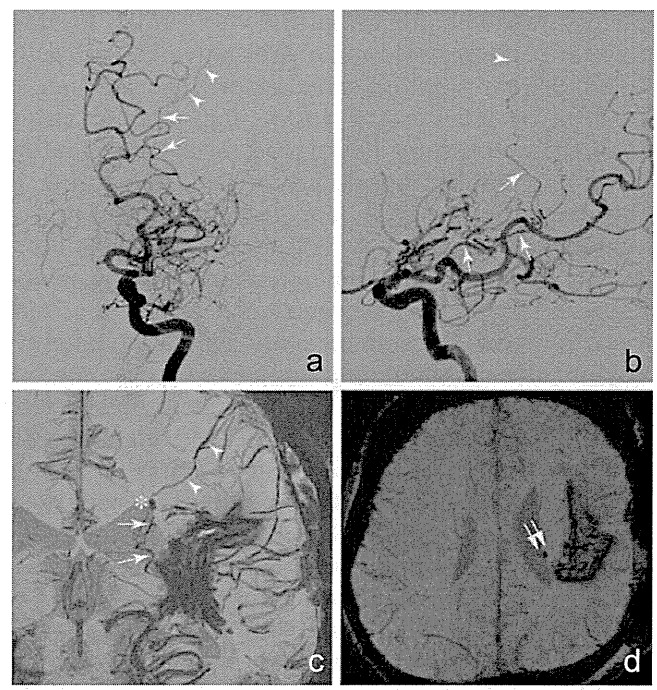

Fig. 4 Periventricular anastomosis originating in the anterior choroidal artery (Case 4). a, b: Anterior-posterior (a) and lateral (b) views of left internal carotid artery angiography showing dilated anterior choroidal artery (*arrows*) connecting to the medullary artery (*arrowhead*). c: Flow-sensitive black-blood magnetic resonance angiography revealing anastomosis (*asterisk*) between the choroidal artery (*arrows*) and the medullary artery (*arrowheads*) located beneath the lateral wall of the atrium. d: Susceptibility-weighted imaging showing the microbleed (*double arrow*) coincident with periventricular anastomosis.

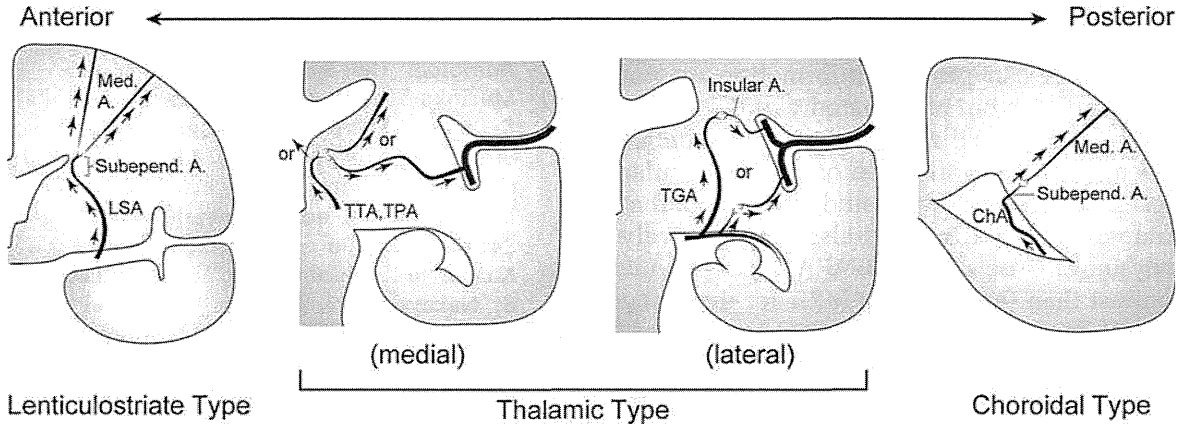

Fig. 5 Schematic illustrations showing a coronal plane of the left cerebral hemisphere and three types of periventricular anastomoses. A.: artery, ChA: choroidal artery, LSA: lenticulostriate artery, Med.: medullary, subepend.: subependymal, TGA: thalamogeniculate artery, TPA: thalamoperforating artery, TTA: thalamotuberal artery.

systemized. Furthermore, these reports focused only on perforating arteries such as lenticulostriate arteries as sources of collaterals. Morioka et al. stressed that abnormal extension or branching of the dilated choroidal artery also served as important collaterals possibly associated with bleeding.[5] Although they did not clearly define the abnormal branches from the choroidal artery, we assumed from observation suggests that the medullary artery represents such branches.

All collaterals described in the present cases share one feature: all anastomosis sites were located in the periventricular area, that is, at the lateral corner of the anterior body of the lateral ventricle (Fig. 1), beneath the ependyma of the third ventricle (Fig. 2), superior to the inferior horn of the lateral ventricle (Fig. 3), and beneath the lateral wall of the atrium of the lateral ventricle (Fig. 4). It might thus be reasonable to classify all these types of anastomoses under one identifier as, say, periventricular anastomosis (Fig. 5).

These anastomoses cluster in the periventricular area possibly because of the presence of the subependymal artery,[10,11] an anatomically hypothesized artery beneath the ependyma and originally described as the ventriculofugal (or centrifugal) artery.[12,13] The subependymal artery might intervene between the perforating and medullary arteries or between the choroidal and medullary arteries in a specific pathological condition such as moyamoya disease. As shown in Fig. 5, periventricular anastomoses can be reasonably classified into three types: lenticulostriate, thalamic, and choroidal. These classifications differ only slightly from those proposed by Kazumata et al.[6] The thalamic type could be subclassified into medial and lateral types according to the location of the anastomosis. The medial thalamic type could also include the connection between the perforating artery and the medial posterior choroidal artery in the roof of the third ventricle, which was not observed in the present series. It might also be acceptable to include in the choroidal classification the possible connection between the medial posterior choroidal artery and pericallosal artery through the corpus callosum, a condition not observed in the present series.

The distribution of periventricular anastomoses corresponds closely to common bleeding sites in moyamoya disease; that is, the basal ganglia, thalamus, temporal stem, and periventricular areas of the entire lateral and third ventricles.[6] This evidence could support the hypothesis that periventricular anastomosis is a surrogate marker for bleeding, a consideration that should be tested in further studies.

II. Clinical importance of FSBB-MRA

FSBB-MRA is a high-resolution black-blood imaging method adequate for visualizing small perforating arteries in the general population and in patients with lacunar infarction.[7] The imaging methods can more sensitively visualize the perforating arteries than time-of-flight MRA.[8] In FSBB-MRA, the signal from rapidly flowing blood in the arteries is attenuated through the application of a very weak motion-probing gradient for signal dephasing, while the signal from slow-moving components, such as the flow in the veins, is much less affected. FSBB-MRA might have two benefits for detecting periventricular anastomoses. First, minimum-intensity projection coronal images with adequate slab thickness noninvasively facilitate visualization of periventricular anastomosis without any effect from numerous vessels overlapping and obscuring the view. Partial volume effect is avoid-

able by simultaneous reading of thin slice source images. Second, unlike conventional angiography, black-blood MRA can provide information on not only the tiny arteries but also anatomy of the parenchymal structure. Visualization of both anatomies seems essential to the evaluation of periventricular anastomoses. Although a recent study illustrated that 3-tesla time-of-flight MRA could also noninvasively depict moyamoya vessels,[14] FSBB-MRA might provide better contrast than time-of-flight MRA for depicting both the collaterals and parenchyma.

In conclusion, this preliminary case series illustrates the potential of FSBB-MRA to reveal abnormal collaterals in moyamoya disease, or moyamoya vessels, characterized as those arising from the lenticulostriate, thalamic perforating, or choroidal arteries and connecting to the medial end of the medullary or insular artery in the periventricular area. The concept of periventricular anastomosis, an alternative definition of moyamoya vessels, might facilitate future optimal grading and classification of moyamoya vessels. The detection of periventricular anastomoses with FSBB-MRA could generate risk estimates of bleeding in moyamoya disease, and larger studies are required.

Acknowledgments

This work was supported by JSPS KAKENHI Grant Number 25461815 and a sponsored research program, "Researches for improvement of MR visualization (No. 150100700014)" provided to Professor Kaori Togashi, Department of Diagnostic Imaging and Nuclear Medicine, Kyoto University Graduate School of Medicine, by Toshiba Medical Systems Corporation, Japan. The authors also thank Ms. Kyoko Takakura for her technical assistance regarding MRI.

Conflicts of Interest Disclosure

The authors report no conflict of interest concerning the materials or methods used in this study or the findings specified in this article.

References

1) Takahashi JC, Miyamoto S: Moyamoya disease: recent progress and outlook. *Neurol Med Chir (Tokyo)* 50: 824–832, 2010
2) Kuroda S, Houkin K: Moyamoya disease: current concepts and future perspectives. *Lancet Neurol* 7: 1056–1066, 2008
3) Cho HJ, Song DB, Choi HY, Heo JH: Lenticulostriate-medullary artery anastomoses in moyamoya disease. *Neurology* 68: E21, 2007
4) Takahashi M: Magnification angiography in moyamoya disease: new observations on collateral vessels. *Radiology* 136: 379–386, 1980
5) Morioka M, Hamada J, Kawano T, Todaka T, Yano S, Kai Y, Ushio Y: Angiographic dilatation and branch extension of the anterior choroidal and posterior communicating arteries are predictors of hemorrhage in adult moyamoya patients. *Stroke* 34: 90–95, 2003
6) Kazumata K, Shinbo D, Ito M, Shichinohe H, Kuroda S, Nakayama N, Houkin K: Spatial relationship between cerebral microbleeds, moyamoya vessels, and hematoma in moyamoya disease. *J Stroke Cerebrovasc Dis* 23: 1421–1428, 2014
7) Okuchi S, Okada T, Ihara M, Gotoh K, Kido A, Fujimoto K, Yamamoto A, Kanagaki M, Tanaka S, Takahashi R, Togashi K: Visualization of lenticulostriate arteries by flow-sensitive black-blood MR angiography on a 1.5 T MRI system: a comparative study between subjects with and without stroke. *AJNR Am J Neuroradiol* 34: 780–784, 2013
8) Gotoh K, Okada T, Miki Y, Ikedo M, Ninomiya A, Kamae T, Togashi K: Visualization of the lenticulostriate artery with flow-sensitive black-blood acquisition in comparison with time-of-flight MR angiography. *J Magn Reson Imaging* 29: 65–69, 2009
9) Kodama N, Suzuki J: Cerebrovascular Moyamoya disease. IIIrd report—the study on the aging of the perforating branches and the possibility of collateral pathway. *Neurol Med Chir (Tokyo)* 14 (pt 1): 55–67, 1974
10) Saito R, Kumabe T, Sonoda Y, Kanamori M, Mugikura S, Takahashi S, Tominaga T: Infarction of the lateral posterior choroidal artery territory after manipulation of the choroid plexus at the atrium: causal association with subependymal artery injury. *J Neurosurg* 119: 158–163, 2013
11) Marinković S, Gibo H, Filipović B, Dulejić V, Piscević I: Microanatomy of the subependymal arteries of the lateral ventricle. *Surg Neurol* 63: 451–458; discussion 458, 2005
12) Van den Bergh R: Centrifugal elements in the vascular pattern of the deep intracerebral blood supply. *Angiology* 20: 88–94, 1969
13) Van den Bergh R: The ventriculofugal arteries. *AJNR Am J Neuroradiol* 13: 413–415, 1992
14) Fushimi Y, Miki Y, Kikuta K, Okada T, Kanagaki M, Yamamoto A, Nozaki K, Hashimoto N, Hanakawa T, Fukuyama H, Togashi K: Comparison of 3.0- and 1.5-T three-dimensional time-of-flight MR angiography in moyamoya disease: preliminary experience. *Radiology* 239: 232–237, 2006

Address reprint requests to: Takeshi Funaki, MD, Department of Neurosurgery, Kyoto University Graduate School of Medicine, 54 Kawahara-cho, Shogoin, Sakyo-ku, Kyoto, Kyoto 606-8507, Japan.
e-mail: tfunaki@kuhp.kyoto-u.ac.jp

JNS

CLINICAL ARTICLE

J Neurosurg 122:400–407, 2015

Unstable moyamoya disease: clinical features and impact on perioperative ischemic complications

Takeshi Funaki, MD,[1] Jun C. Takahashi, MD, PhD,[1] Yasushi Takagi, MD, PhD,[1] Takayuki Kikuchi, MD, PhD,[1] Kazumichi Yoshida, MD, PhD,[1] Takafumi Mitsuhara, MD, PhD,[1] Hiroharu Kataoka, MD, PhD,[2] Tomohisa Okada, MD, PhD,[3] Yasutaka Fushimi, MD, PhD,[3] and Susumu Miyamoto, MD, PhD[1]

Departments of [1]Neurosurgery and [3]Diagnostic Imaging and Nuclear Medicine, Kyoto University Graduate School of Medicine, Kyoto; and [2]Department of Neurosurgery, National Cerebral and Cardiovascular Center, Osaka, Japan

OBJECT Unstable moyamoya disease, reasonably defined as cases exhibiting either rapid disease progression or repeated ischemic stroke, represents a challenge in the treatment of moyamoya disease. Despite its overall efficacy, direct bypass for such unstable disease remains controversial in terms of safety. This study aims to reveal factors associated with unstable disease and to assess its impact on postoperative silent or symptomatic ischemic lesions.

METHODS This retrospective cohort study included both pediatric and adult patients with moyamoya disease who had undergone 140 consecutive direct bypass procedures at Kyoto University Hospital. "Unstable moyamoya disease" was defined as either the rapid progression of a steno-occlusive lesion or repeat ischemic stroke, either occurring within 6 months of surgery. The extent of progression was determined through a comparison of the findings between 2 different MR angiography sessions performed before surgery. The clinical variables of the stable and unstable disease groups were compared, and the association between unstable disease and postoperative diffusion-weighted imaging (DWI)–detected lesion was assessed through univariate and multivariate analyses with generalized estimating equations.

RESULTS Of 134 direct bypass procedures performed after patients had undergone at least 2 sessions of MR angiography, 24 (17.9%) were classified as cases of unstable disease. Age younger than 3 years ($p = 0.029$), underlying disease causing moyamoya syndrome ($p = 0.049$), and radiographic evidence of infarction ($p = 0.030$) were identified as factors associated with unstable disease. Postoperative DWI-defined lesions were detected after 13 of 140 procedures (9.3%), although only 4 lesions (2.9%) could be classified as a permanent complication. The incidence of postoperative DWI-detected lesions in the unstable group was notable at 33.3% (8 of 24). Univariate analysis revealed that unstable disease ($p < 0.001$), underlying disease ($p = 0.028$), and recent stroke ($p = 0.012$) were factors associated with DWI-detected lesions. Unstable disease remained statistically significant after adjustment for covariates in both the primary and sensitivity analyses (primary analysis: OR 6.62 [95% CI 1.79–24.5]; sensitivity analysis: OR 5.36 [95% CI 1.47–19.6]).

CONCLUSIONS Unstable moyamoya disease, more prevalent in younger patients and those with underlying disease, is a possible risk factor for perioperative ischemic complications. Recognition of unstable moyamoya disease may contribute to an improved surgical result through focused perioperative management based on appropriate surgical risk stratification.

http://thejns.org/doi/abs/10.3171/2014.10.JNS14231

KEY WORDS moyamoya disease; rapid progression; cerebral revascularization; intraoperative complication; vascular disorders

A MAJOR characteristic of moyamoya disease is the chronic progression of stenosis in the terminal portion of the internal carotid artery (ICA).[24] The rate of this progression varies by patient. Angiographic progression can occur in one-half of pediatric patients and one-quarter of adult patients,[19,21] while angiographic findings in the remaining patients are stable for years. Some patients demonstrate extremely rapid progression from disease onset, resulting in poor outcome.[4,17,18] Fujiwara et al. and Kim et al. reported similar cases in which rapid an-

ABBREVIATIONS ACA = anterior cerebral artery; DWI = diffusion-weighted imaging; GEE = generalized estimating equation; ICA = internal carotid artery; MCA = middle cerebral artery; MRA = MR angiography; mRS = modified Rankin Scale; PCA = posterior cerebral artery; STA = superficial temporal artery; TIA = transient ischemic attack.

SUBMITTED January 31, 2014. **ACCEPTED** October 21, 2014.

INCLUDE WHEN CITING Published online November 28, 2014; DOI: 10.3171/2014.10.JNS14231.

DISCLOSURE The authors report no conflict of interest concerning the materials or methods used in this study or the findings specified in this paper.

giographic progression resulted in fatal outcome.[4,18] Kim et al. reported that younger patients were more likely to suffer from an aggressive clinical course, of whom a substantial number experienced repeat stroke.[17]

While the impact of such unstable disease on clinical outcome is receiving more focused attention, few studies have attempted to clearly define this condition. Accurate risk stratification in moyamoya disease requires objective definition of disease instability. According to the articles mentioned above,[4,17,18] disease progression and repeat stroke are considered essential factors reflecting instability of moyamoya disease. The concept of unstable moyamoya disease defined as either rapid disease progression or repeat stroke seems reasonable, considering that unstable angina pectoris, the concept representing instability of angina pectoris, is also characterized as an exacerbating or recurrent symptom with rapid progression of stenosis in the coronary artery.[1,23,27]

Treatment of unstable moyamoya disease is challenging because patients with the disease commonly develop stroke during the perioperative period or even while awaiting surgery.[7,17] Direct bypass, such as superficial temporal artery–to–middle cerebral artery (STA-MCA) bypass, has the advantage of contributing to increased cerebral blood flow soon after surgery.[10] The safety and efficacy of direct bypass for unstable disease are, however, controversial.[7,17]

This retrospective cohort study had 2 objectives: to detect clinical factors associated with unstable moyamoya disease and to determine whether the presence of such instability is associated with postoperative silent or symptomatic ischemic lesions detected on diffusion-weighted imaging (DWI).

Methods

This study was approved by the ethics committee of the Kyoto University Graduate School of Medicine.

Selection Criteria

A total of 88 pediatric and adult patients with moyamoya disease underwent 148 revascularization surgeries at Kyoto University Hospital between 2009 and 2013. The inclusion criteria for the present study were as follows: diagnosis of moyamoya disease or moyamoya syndrome; patients who underwent direct revascularization at Kyoto University Hospital in 2009 or thereafter; and patients who underwent routine postoperative DWI no longer than 14 days after surgery.

Diagnoses were made according to the criteria proposed by the Research Committee on Moyamoya Disease in Japan.[24] "Moyamoya syndrome" is defined as a secondary moyamoya phenomenon caused by an underlying disease such as an autoimmune disease, meningitis, brain tumor, hyperthyroidism, Down syndrome, neurofibromatosis Type 1, or a history of head irradiation.[24] The present study also included unilateral disease in which only 1 side of the ICA was involved. "Direct bypass" was defined as a direct anastomotic procedure including STA-MCA, STA–anterior cerebral artery (ACA), and occipital artery–posterior cerebral artery (PCA) bypasses.

Of the 148 consecutive revascularization procedures, 3 were excluded because they involved only indirect bypass in the ACA territory. Although postoperative MRI with DWI was mandatory in our treatment protocol, postoperative DWI was not performed after 5 procedures (these cases were excluded from the study) because a postoperative MRI scan was performed but no DWI was acquired (4 procedures), and because no MRI was performed since the patient sought early discharge (1 procedure). None of these 5 patients presented with a new neurological deficit after surgery. Consequently, 140 procedures conducted in 86 patients were included in the present study (Fig. 1).

Variables

Unstable moyamoya disease, a primary variable of interest, was defined as a condition with evidence of either rapid stenosis progression or repeated stroke. "Rapid stenosis progression" was defined as progression of a steno-occlusive lesion in an ICA, ACA, MCA, or PCA that had occurred within 6 months (Fig. 2). Whether the progression had occurred was determined using an MR angiography (MRA) scoring system,[8] and the scores were compared between 2 different sessions performed before surgery. Almost all patients referred to our institution had already undergone MRA, the results of which could be used as control imaging. If only 1 imaging session had been performed before surgery, or if the interval between the 2 sessions was less than 2 weeks, the data were eliminated from further analysis. Decreased antegrade flow due to bypass in the ipsilateral MCA territory was not regarded as stenosis progression. "Repeat stroke" was defined as newly developed symptomatic infarctions confirmed on DWI and occurring at least twice during an interval not exceeding 6 months.

The other variables possibly affecting surgical outcome were identified from previous literature: age younger than 3 years,[16] female sex,[15] presence of underlying disease causing moyamoya syndrome,[6,22] transient ischemic attacks (TIAs) occurring at a frequency exceeding 3 times per month,[16] radiographic evidence of preexisting infarc-

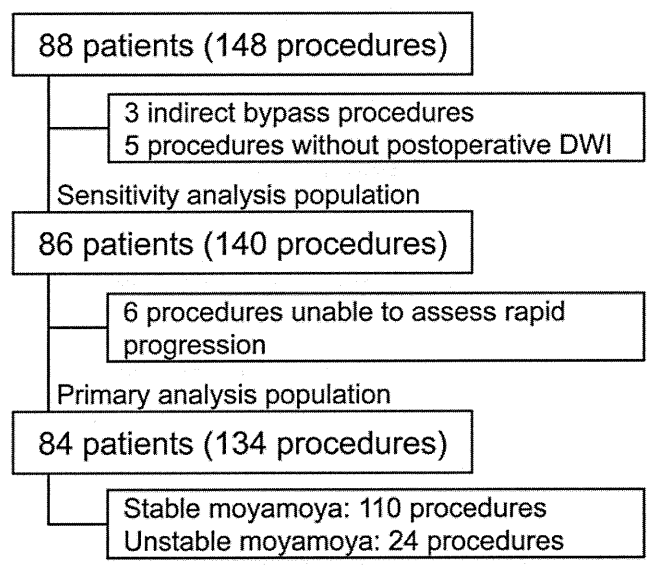

FIG. 1. Flowchart for patient inclusion.

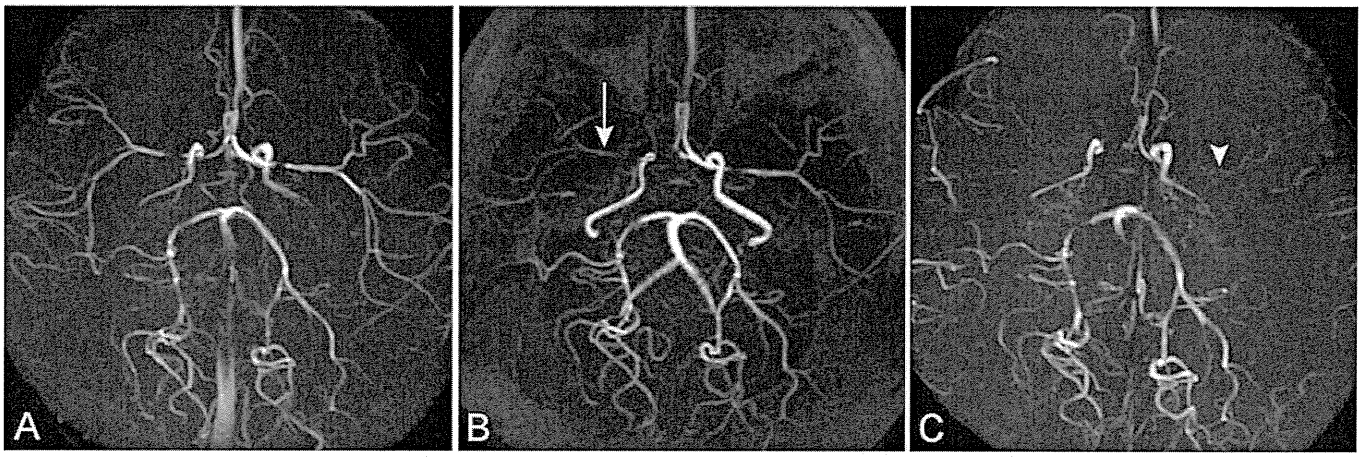

FIG. 2. Serial MRA images obtained in a 1-year-old boy representing rapid disease progression. **A:** Image obtained 2 months before referral to our hospital, revealing moderate stenosis in the terminal portion of the ICA and M_1 segment of the MCA bilaterally. **B:** Image obtained at admission to our hospital, revealing signal decrease in the right MCA compared with that obtained 2 months previously, suggesting rapid disease progression in the right MCA. The patient subsequently underwent direct bypass for the right MCA territory. **C:** Image obtained 2 months after surgery, revealing an invisible signal in the left MCA, suggesting rapid disease progression in the left MCA.

tion,[9,16,25] recent stroke occurring no more than 6 weeks before surgery or evidence of recent stroke on preoperative DWI,[9,16] advanced stage moyamoya (Suzuki Stages IV, V, and VI) in the ICA,[11] and disease involvement in the PCA.[11] "Unilateral disease" was defined as unilateral stenosis or occlusion of the terminal portion of the ICA with the formation of moyamoya vessels accompanied by no lesion or a subtle lesion around the contralateral terminal portion of the ICA. "Severe hemodynamic compromise" was defined as a defect in the cerebral blood flow both at rest and after acetazolamide challenge revealed on SPECT. Administration of antiplatelet agents was also recorded.

Surgery

All patients underwent MRI, SPECT, and angiography before surgery. Surgical revascularization was indicated for patients with cerebral ischemic manifestation. Patients presenting with other symptoms, such as epilepsy and intracranial hemorrhage, were also considered candidates for surgical revascularization as long as hemodynamic compromise existed. All patients underwent direct bypass, STA-MCA anastomosis, or combined bypass comprising STA-MCA anastomosis and encephalo-myo-synangiosis as a first-line treatment.[13] After completing 2 sessions of revascularization for the MCA territories, some patients required additional revascularization surgeries for the ACA and PCA territories. Our surgical procedures and treatment protocol are described in previous literature.[5,12,13] Antiplatelet agents, if administered, were discontinued for 3 days before surgery and 2 days after surgery.

During general anesthesia, $PaCO_2$ and end-tidal CO_2 were closely monitored, and the level of $PaCO_2$ was strictly maintained between 37 and 40 mm Hg.

Outcome

All silent and symptomatic ischemic lesions, a primary outcome in this study, were diagnosed by neuroradiologists based on the results of DWI performed no longer than 14 days after surgery. A symptomatic lesion was defined as one causing a decline in the modified Rankin Scale (mRS) score. Such lesions were classified into either of 2 categories: cortical infarction or subcortical infarction. The patency of the bypass was also assessed using MRA performed in the same imaging session.

Statistical Analysis

Since more than half of the patients underwent multiple procedures, postoperative outcomes for such patients might not be statistically independent. In consideration of these dependencies, we used the generalized estimating equation (GEE) approach for the demographic descriptions of stable and unstable moyamoya disease as well as univariate and multivariate logistic regression analyses.[2] All p values and confidence intervals were calculated with robust standard error estimates from the GEE approach with the independent working correlation structure.

Because of rare outcome events, we selected preoperative variables only with p values < 0.05 as covariates adjusted for the multivariate GEE logistic analysis. In light of its clinical importance, radiographic evidence of infarction was incorporated into the multivariate analysis regardless of its p value. As mentioned in *Results*, assessment of disease progression was not possible for 6 procedures; hence, these procedures were excluded from the primary analysis. We also conducted a sensitivity analysis that included the 6 procedures, all of which were assumed to be those of unstable disease (Fig. 1), considering the possibility that such patients might undergo only 1 MRA session because of rapid progression. We fit the same GEE logistic regression for both the primary and sensitivity analyses. Two-sided values of $p < 0.05$ and 95% confidence intervals of odds ratios that do not include 1 were considered significant. All analyses were performed using JMP (version 9) software and Windows SAS (version 9.3, SAS Institute Inc.).